X-PEEM Study on Surface Orientation of Stylized and Rubbed Polyimides

A. Cossy-Favre,*,†,‡ J. Díaz,† Y. Liu,§ H. R. Brown,|| M. G. Samant,⊥ J. Stöhr,⊥ A. J. Hanna,† S. Anders,† and T. P. Russell§

Advanced Light Source, Lawrence Berkeley National Laboratory, 1 Cyclotron Road, Berkeley, California 94720, Department of Polymer Science and Engineering, University of Massachusetts, Amherst, Massachusetts 01003, BHP Steel Institute, University of Wollongong, Wollongong NSW 2522, Australia, and Almaden Research Center, IBM Research Division, San Jose, California 95120

Received January 8, 1998

ABSTRACT: X-ray photoelectron emission microscopy (X-PEEM) was used to study the surface orientation of stylized and rubbed polyimide thin films. Using soft X-rays produced by a synchrotron light source, this technique combines high spatial resolution imaging with near-edge X-ray absorption fine structure (NEXAFS) spectroscopy to yield information on the surface orientation of the films. Stylizing is an ideal model of the rubbing process since the local stress acting on the polyimide to orient the molecules can be calculated. The minimum normal stress necessary to orient the surface of BPDA−PDA films was found to be 45 MPa much lower than the bulk yield stress of 200−300 MPa. Studies of the polyimide films oriented by the conventional rubbing method showed lateral inhomogeneities in the orientation of the polymer at the surface.

Introduction

Thin (≈0.2 μm) films of an aromatic polyimide, which were coated onto the electrode surfaces and were in contact with a liquid crystal, are essential components in flat panel displays. After deposition, the polyimide film is unidirectionally rubbed with a velour cloth.[1] Liquid crystals, in contact with the rubbed surface, form a monodomain aligned parallel to the direction of the rubbing.[2,3] Numerous studies have been carried out to understand the mechanism responsible for the alignment of the liquid crystal molecules on such surfaces, and several mechanisms have been proposed, including microgrooves on the surface formed during rubbing[4] or polar interactions between the liquid crystals and oriented polymer molecules which serve as a molecular template.[2,5] The second mechanism has emerged as the most likely. However, the effect of the rubbing process on polyimide chains is still poorly understood. Grazing incidence X-ray scattering studies on BPDA−PDA clearly demonstrated that the polyimide chains near the surface were markedly aligned during the rubbing[6] process despite the rather small load applied during rubbing (2 g/cm^2). The origin of the relative facility to orient the chains at the surface of polymers films suggests that the mechanical properties at the surface are different from those of the bulk.[7−12]

Near-edge X-ray absorption fine structure (NEXAFS) has been shown to be a unique tool to probe the surface structure and bulk orientation of polymer films.[13,14] Near the K-shell absorption threshold, NEXAFS spectra are dominated by resonances arising from transitions from the 1s core level to unfilled molecular orbitals of π^* and σ^* symmetry. Since such states are specific to the bonding within different functional groups, NEXAFS can be used to probe the chemical composition of polymers.[15,16] The intensity of the NEXAFS resonances depends on the nature and filling of the molecular orbitals and on the included angle between the electric field vector of the X-rays $\vec{E}$ and the direction of the valence orbital.[17] The use of nearly linearly polarized light produced by a synchrotron enables one to access the orientation of chain segments near the surface. For an oriented specimen, the intensity depends on the orientation of $\vec{E}$, with respect to the deformation direction. The difference in the intensities yields a dichroic ratio[14] which can be calculated to quantify the degree of orientation of the polymer chains.

By comparing the C K-edge detection NEXAFS signal from the surface (10 Å sampling depth) obtained by Auger electron yield (AEY) detection to the signal from the near surface region (100 Å) obtained by total electron yield (TEY) detection, Samant et al.[14] confirmed that the polyimide chains are aligned along the rubbing direction and that the alignment of the polyimide is largest at the surface and decays into the bulk over a depth of about 100 Å. After the rubbing, the phenyl ring planes align preferentially parallel to the rubbing direction. The surface orientation saturated at relatively small loads of 2 g/cm^2 and rubbing distances of 300 cm. These values represent an average of the orientation over the entire surface of the sample. The rubbing process is, however, poorly defined since the number of fibers in contact with the surface and the shape of the fibers during contact are unknown. The actual stress applied by the tip of the fiber onto the polyimide chains is still unknown. Kikuchi et al.[18] predicted limiting values of the stress of a few MPa to over 300 MPa. This estimate is of little value since it spans a range including the bulk yield stress value of 200−300 MPa.

† Lawrence Berkeley National Laboratory.
‡ Present address: EMPA, Überlandstrasse 129, 8600 Dübendorf, Switzerland. Telephone: + 41/1 823 43 48. Fax +41/1 821 62 44.
§ University of Massachusetts.
|| University of Wollongong.
⊥ IBM Research Division.

S0024-9297(98)00029-1 CCC: $15.00
Published on Web 07/03/1998

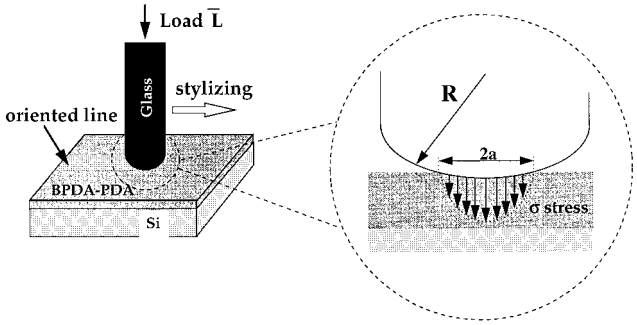

Figure 1. Schematic of the stylizing process. The light-shaded parallelepiped represents the Si wafer on top of which the polyimide layer has been spin coated (dark-shaded parallelepiped). A glass lens is rubbed across the polyimide film creating a track of oriented chains of width 2*a*. The glass lens tip has a curvature radius R and is pressed on the polyimide with a force $\vec{L}$. The local stress σ across the track is ellipsoidal.[23]

Hence we use a stylus of a known geometry to induce alignment. The contact area of a stylus is about 10 μm, and therefore we need to monitor the NEXAFS intensity with $\approx$1 μm lateral resolution. Spectromicroscopy techniques, such as scanning transmission X-ray microscopy (STXM),[13,15] have already demonstrated their usefulness in studying the lateral chemical homogeneity of polymer thin films. However to obtain a sensitivity of only 100 Å from the surface, X-ray photoelectron emission microscopy, X-PEEM, is more useful. Since in a X-PEEM microscope only low-energy secondary electrons are detected, information similar to that of the TEY in conventional NEXAFS is obtained.[19]

Herein X-PEEM is used to study the orientation of thin polyimide films that have been rubbed or oriented using a stylus of well-defined shape with a known load. The stylizing process is used as a model case to correlate the polymer orientation with the precisely known local stress on the film. Micro-NEXAFS spectra recorded of regions within a stylized line are compared to the results of previous conventional NEXAFS experiments on rubbed samples. Furthermore the PEEM study is extended to rubbed polyimides, similar to those used in actual flat panel displays, showing the lateral inhomogeneity of the rubbing process.

Experimental Section

Films of poly(biphenyltetracarboxylic dianhydride-*p*-phenylenediamine) polyimide (BPDA−PDA) were prepared by spin coating solutions of the corresponding amic acid ester in *N*-methylpyrrolidinone onto 1 in. diameter Si ⟨100⟩ wafers. The film thickness was 1300 Å. The amic acid ester films were then heated to 80 °C to remove the solvent. The samples were transferred to a hot plate and gradually heated to 300 °C under flowing nitrogen to cycloimidize the polymer. After cooling to room temperature the samples were stylized as shown in Figure 1. A glass lens of radius $R = 9.81$ mm, was attached to one end of a double cantilever, which is mounted on a strain gauge at the other end. The lens was rubbed across the surface of the polyimide film with a load $\vec{L}$ of 2.70×10^{-2}N over a distance of 1 cm. The average friction over the rubbing distance is 2.02×10^{-2}N, which corresponds to an average friction coefficient of 0.75. Other samples were rubbed by passing a velour cloth over the film using a constant load of 2 g/cm^2 over 300 cm as described previously.[6,14]

A polymer chain is schematically represented in Figure 2a and a partial sequence of its chain is shown in Figure 2b. One monomer unit is defined as the BPDA−PDA repeat unit (dashed box). All the atoms in a BPDA unit define a plane.[14] For a fully stretched chain[20] the axes of the monomers are parallel to the chain axis and the PDA units are rotated at an angle of $\delta = 60°$ with respect to the BPDA units; see Figure 2c. When the samples are rubbed, the chains are not fully stretched; instead, they preferentially align along the rubbing direction. The phenyl rings as well as the C=O bonds lie preferentially within the plane parallel to the sample surface.

The X-PEEM measurements were performed at the Stanford Synchrotron Radiation Laboratory (SSRL) on beam line 10-1, which delivers soft X-ray radiation from a 15 period wiggler. This beam line is equipped with a spherical grating monochromator. The entrance and exit slits were set to 80 μm, to obtain the maximum photon flux on the sample without destroying the polyimide chains. The energy resolution at $h\nu = 300$ eV is 250 meV. The photocurrent of a high-transmission (85%) grid freshly coated with Au served as the reference signal to normalize the data. A typical Au photocurrent of 1 nA was obtained at these slits settings for a storage ring current of 60 mA at $h\nu = 350$ eV.

The experimental geometry is displayed in Figure 3. The sample surface was defined by the $x-y$ plane, while the surface normal was along the z axis. Experiments were performed with the $\vec{E}$ vector parallel and perpendicular to the rubbing direction. The photon beam impinged onto the sample in the $x-z$ plane in the *X*-geometry (or perpendicular geometry), Figure 3a, and in the $y-z$ plane in the *Y*-geometry (or parallel geometry), Figure 3b. In both *X*- and *Y*-geometries, the photon beam incidence angle was $\vartheta = 30°$ with respect to the sample surface. The X-ray beam was elliptically polarized with a degree of linear polarization $P = 0.87$.[14] The X-PEEM optical axis was along the z direction.

The X-PEEM is a simple, two electrostatic lens, imaging system.[21,22] The photoemitted electrons were accelerated into the electron optics with 10 kV accelerating voltage. The image was intensified through a multichannel plate and was projected onto a phosphor screen. A data acquisition system equipped with a Sony camera Type XC-73 was used to acquire images and to record NEXAFS spectra in the areas selected within the field of view. A typical image consisted of an average over 750 frames with an acquisition time of 10 ms/frame, and a typical NEXAFS spectrum was acquired as an average over 30 frames per energy point.

Images as acquired by the X-PEEM for different excitation energies look like parts a−c of Figure 4, for example. To get the normalized version of these images we apply the following mathematical procedure: First, image a is subtracted from images b and c to remove the preedge background. Then the normalized image (in our case the image in Figure 5a) is obtained from the background subtracted image b divided by the background subtracted image c.

Micro-NEXAFS spectra were acquired from areas of 2 μm $\times$ 10 μm selected on the PEEM images by collecting the integrated intensity of the images within the selected region as function of the excitation energy. The spectra were then normalized by the reference signal from the Au grid. After subtraction of a linear preedge background function, the spectra were renormalized to a constant edge jump, arbitrarily set to 1, far above the edge.

Results

Stylized Lines. In Figure 4, measured images are shown where a stylized line is oriented parallel to the electric field $\vec{E}$ of the incident X-ray beam. Images a−c of Figure 4 were taken at photon energies of 283.7, 285.3, and 349.7 eV, respectively. No normalization was applied to these images. Figure 5a is a normalized version of Figure 4b, and Figure 5b is a normalized image from the other half of the sample with the stylized line oriented perpendicular to the electric field vector $\vec{E}$. Figure 6 shows normalized micro-NEXAFS spectra acquired from the stylized lines. The full curve represents the spectrum taken within the line oriented parallel to $\vec{E}$, while the dotted line is the spectrum from the line perpendicular to $\vec{E}$. As discussed before, the

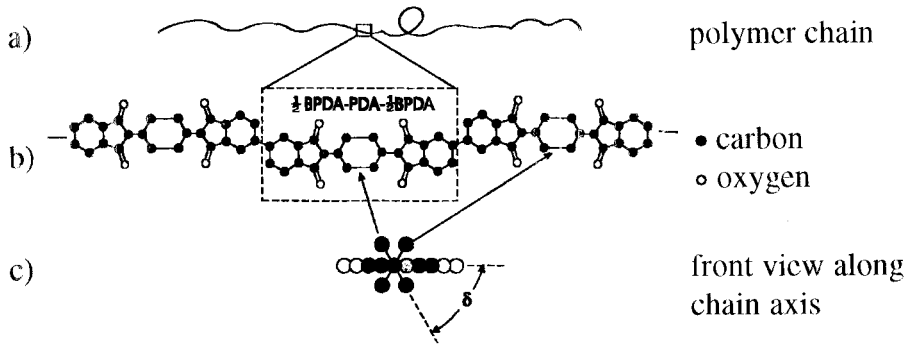

Figure 2. (a) Schematic representation of a polymer chain. (b) Chemical structure of BPDA−PDA polyimide in the fully stretched configuration. The solid dots (●) represent carbon atoms while the open dots (○) represent the oxygen atoms. In this case the chain axis is parallel to the monomer axis and the π^* orbitals of all phenyl rings and the C=O units are perpendicular to the chain axis. (c) View of the fully stretched polyimide chain along the chain axis, showing that the plane of the PDA groups is rotated about the chain axis by $\delta = 60°$ relative to the plane of the BPDA groups.

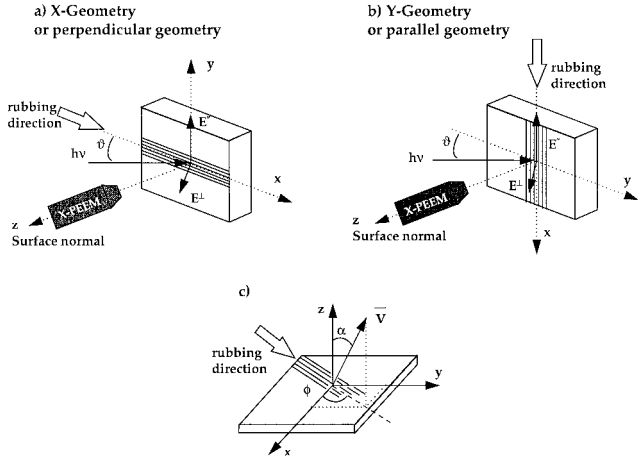

Figure 3. Coordinate system describing the experimental geometry. Axes x and y define the sample surface plane and axis z defines the sample normal. The sample is stylized along the x direction. The X-PEEM optical axis is along the z direction. (a) *X*-Geometry: The X-rays are incident in the $x-z$ plane, along the x direction, at an angle $\theta = 30°$ with respect to the sample surface plane $x-y$. The electric field vector of the circularly polarized light has two components, $E^{\parallel}$ (major) and $E^{\perp}$. The major component $E^{\parallel}$ which lies along the y axis is perpendicular to the rubbing direction therefore this geometry is also called *perpendicular geometry*. $E^{\perp}$ lies in the $x-z$ plane at an angle $\vartheta = 30°$ with the z axis. (b) *Y*-Geometry: The photon beam axis lies in the $y-z$ plane, along the y direction, at an angle $\theta = 30°$ with respect to the sample surface plane $x-y$. The major component $E^{\parallel}$ which lies along the x axis is parallel to the rubbing direction; therefore, this geometry is also called *parallel geometry*. $E^{\perp}$ lies in the $y-z$ plane at an angle $\vartheta = 30°$ with the z axis. (c) Specification of the π bond direction of the phenyl in the polyimide chains characterized by a vector $\vec{V}$, in terms of a polar angle α and azimuthal angle ϕ relative to the sample coordinate system.

micro-NEXAFS measured with the X-PEEM[19] correspond to TEY NEXAFS spectra with a sampling depth of about 100 Å.[14] Inset 1 of Figure 6 is an enlarged section of Figure 6 showing the three characteristic maxima of the π^* resonance at 285.3, 286.5, and 287.7 eV associated with specific C atoms[14] as indicated in inset 2.

In Figure 4, the stylized line is visible at the π^* resonance of the phenyl ring but not below or above the C K-absorption edge. This indicates that the contrast obtained in Figure 4b is not topological in nature. AFM measurements performed on the same sample confirm this statement since no topological traces of the stylized lines were observed. Note that the contrast in Figure 4b is small. The image intensity is strongly modulated by the nonconstant X-ray intensity across the field of view. It is therefore necessary to normalize the image as shown in Figure 5, to eliminate the inhomogeneity. The stylized lines appear black on a gray back ground (Figure 5a) when the line is parallel to the electric field vector $\vec{E}$ and white on a gray background when the line is perpendicular to $\vec{E}$ (Figure 5b). This inversion of contrast when the stylized line is rotated by 90° shows that the contrast is not of chemical origin, but it is a polarization effect due to orientation of the phenyl π^* orbitals. If the contrast were of chemical nature it would be independent of the sample orientation. The origin of the polarization contrast is shown in Figure 6. The phenyl π^* resonnance at 285.3 eV is seen to be larger for $\vec{E}$ perpendicular than parallel to the stylized line. Hence in Figure 5 the line is white (higher electron yield) for $\vec{E}$ perpendicular and black (lower electron yield) for $\vec{E}$ parallel to the stylized line. The analysis of images and micro-NEXAFS spectra taken at the π^* resonance of the O K-absorption edge show the same effect. The spectra shown in Figure 6 are similar to those obtained in conventional NEXAFS measurements.[14]

Dichroic Ratio. With the stylus the chains are aligned along the stylizing direction in a manner similar to that observed in the rubbing process described in the paper from Samant et al.[14] The phenyl ring π^* bonds preferentially lie in a plane normal to the chain axis. Before the dichroic ratio from our data is compared with the one obtained on rubbed samples,[14] the expression of the dichroic ratio is translated in our geometry to correspond to the definition from Samant et al. (see Figure 3). The angular dependence of the measured NEXAFS intensities is governed by the following general equation:[17]

$$I_i = PI_i^{\parallel} + (1 - P)I_i^{\perp} \tag{1}$$

Here, $i = x$, y, and $I^{\parallel}$ and $I^{\perp}$ are the intensities corresponding to the parallel and perpendicular components of the $\vec{E}$ vector, as illustrated in Figure 3. In our geometry the equations for the NEXAFS intensities[17] are

$$I_x^{\parallel} = C \sin^2 \alpha \sin^2 \phi \tag{2}$$

$$I_y^{\parallel} = C \sin^2 \alpha \cos^2 \phi \tag{3}$$

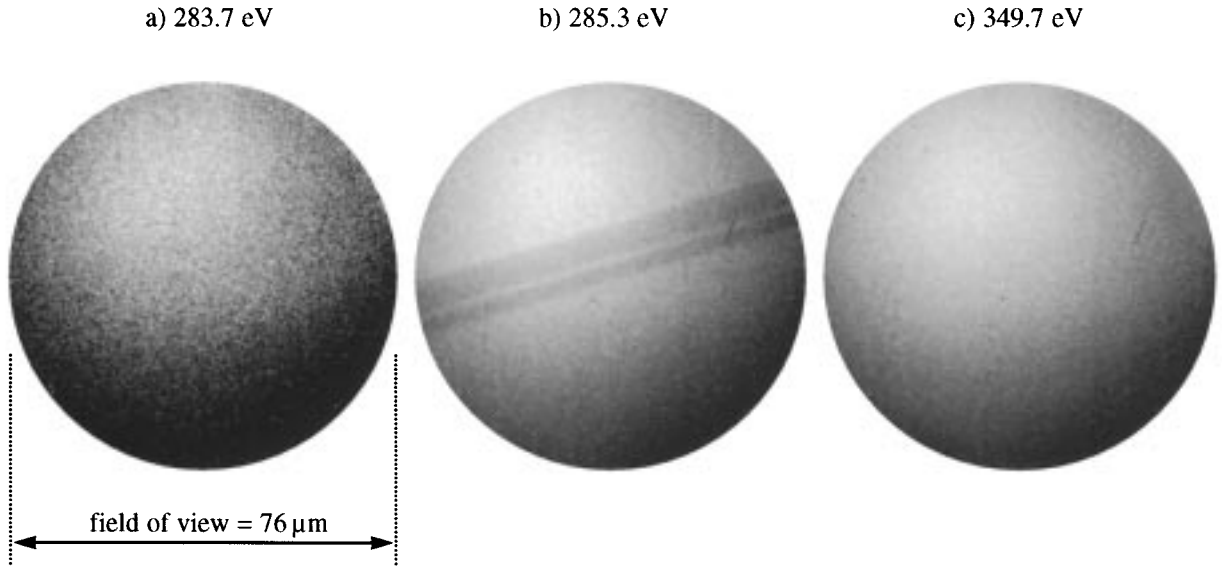

Figure 4. As-measured X-PEEM images of a stylized line (dark) oriented parallel to the X-ray electric field vector $\vec{E}$. (a) at 283.7 eV; (b) at 285.3 eV; (c) at 349.7 eV. The field of view is 76 μm for all three pictures. The thin bright line along the stylized line is probably due to a dust particle caught between the lens and the polyimide film. Within this thin line, the polyimide film is not oriented since the intensity is the same as in the nonoriented area outside the stylized line. The brighter region in the upper left of the images is due to a inhomogeneity in the photon beam intensity.

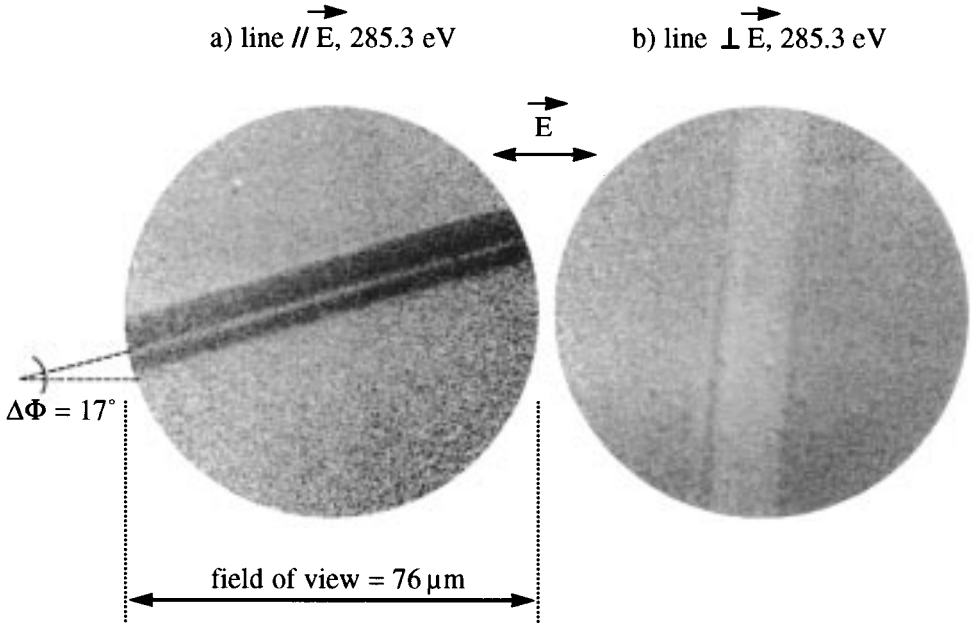

Figure 5. Normalized X-PEEM images, of the line oriented (a) parallel to $\vec{E}$ and (b) perpendicular to $\vec{E}$, recorded at 285.3 eV. The line appears black on the gray background of nonoriented chains in part a and white on the gray background in part b, as proof of a pure orientation contrast. Note in part a that the stylized line is not directed exactly parallel to $\vec{E}$, but an offset angle ϕ of 17° is measured between $\vec{E}$ and the line. This offset angle is taken into account to calculate the dichroic ratio (see text). In part b the line is also not completely perpendicular to $\vec{E}$, but this small offset angle of 3° is neglected.

$$I_x^{\perp} = C\,[\cos^2\alpha\cos^2\vartheta + \sin^2\alpha\sin^2\vartheta\cos^2\phi] \quad (4)$$

$$I_y^{\perp} = C\,[\cos^2\alpha\cos^2\vartheta + \sin^2\alpha\sin^2\vartheta\sin^2\phi] \quad (5)$$

where C is a constant and α, ϑ, and ϕ are defined in Figure 3.

The dichroic ratio defined by Samant et al.[14] and further translated for our geometry has the following form:

$$R_{xy} = (I_y - I_x)/[(I_x + I_y)(2P - 1)] \quad (6)$$

I_x and I_y represent micro-NEXAFS intensities within the stylized line at 285.3 eV, for the line perpendicular respectively parallel to the electric field vector $\vec{E}$. I_x = 0.91 and I_y = 1.14 according to the micro-NEXAFS spectra, Figure 6. As shown in Figure 5a, the stylized line is not exactly oriented parallel to the field vector $\vec{E}$ but an offset angle of $\Delta\phi$ = 17° is measured between the line and $\vec{E}$ (we neglected the offset angle of 3° in the perpendicular geometry). Our experimental value of I_y must therefore be corrected to obtain the exact value of I_y. First we extract the value of ϕ from the experimental ratio I_x/I_y by replacing ϕ by $\phi - \Delta\phi$ in the eqs 1−5. We obtain ϕ = 49° which is close to the value of 50.4° obtained by Samant et al.[14] We obtain the

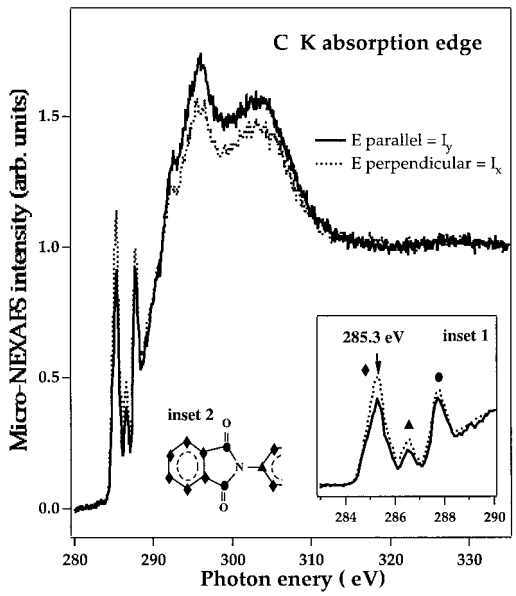

Figure 6. Micro-NEXAFS spectra from an area within the stylized lines for the lines parallel (full curve) and perpendicular (dotted curve) to the electric field vector $\vec{E}$. The data have been normalized as discussed in the text. Inset 1 shows the π^* resonance at an enlarged scale. The three intensity maxima at 285.3, 286.5 and 287.7 eV correspond to phenyl C atoms (diamonds), phenyl C atoms with bonds to N (triangles), and carbonyl carbon atoms (circles), respectively. Inset 2 is a schematic representation of the BPDA−PDA molecule.

corrected value $I_y = 0.68$ (assuming a polarization $P = 1$). and a dichroic ratio value of $R_{xy} = -0.21$, using eq 6. This value of R_{xy} corresponds to the saturation value of $R_{xy} = -0.2$ obtained from TEY data on samples rubbed with a load of 2 g/cm^2 over 300 cm.[14]

Minimum Normal Stress. From the width of the stylized lines measured with the X-PEEM, it is possible to estimate the minimum normal stress necessary to orient the polyimide chains, using the Hertzian theory of contact stress [23,24] under the assumption that the BPDA−PDA film is too thin to accommodate any depression under the load $\vec{L}$ (Hooke's law). The polyimide film is neglected and the depression is assumed to be in the Si substrate. The radius of the contact, a, as described in Figure 1 is

$$a = 3RL/4\pi(k_1 + k_2) \tag{7}$$

where $k_i = (1 - \nu_i^2)/\pi E_i$. E_i is the elastic modulus of the glass lens (70G Pa) or that of the Si substrate (107 Gpa). ν_i is the poisson ratio of the glass (0.3) or that of the Si substrate (0.3). R (9.81 mm) is the radius of the glass lens. $\vec{L}$ (2.7×10^{-2} N) is the load applied for stylizing. The radius of contact ($2a$) of the lens obtained from eq 7 is 16 μm. According to the Hertzian theory the normal stress across the contact is ellipsoidal. For a central stress of $\sigma_0 = 3L/2\pi a^2$, the stress at a position r is

$$\sigma = \sigma_0 (1 - (r/a)^2)^{1/2} \tag{8}$$

The width of the stylized line determined from Figure 5 is 12 μm ($2r$). The stress σ applied at the edge of the line (i.e. for $r = 6$ μm) is $\sigma = 45$ MPa using eq 8. Since the measured friction coefficient is 0.75, the minimum shear stress necessary to orient the polyimide chains at the surface of the BPDA−PDA films is therefore 34 MPa. Our value of 45 MPa for the minimum normal stress necessary to orient the BPDA−PDA chains lies between the estimated values of a few megapascals and the 300 MPa of Kikuchi et al.[18] The much larger bulk yield stress of 200−300 MPa indicates that the mechanical properties at the surface of the polyimide films are markedly different from those of the bulk.

In the discussion so far it has been assumed that the surfaces of the lens and the polymer are sufficiently smooth such that the real contact area is equal to the nominal contact area. The validity of this assumption

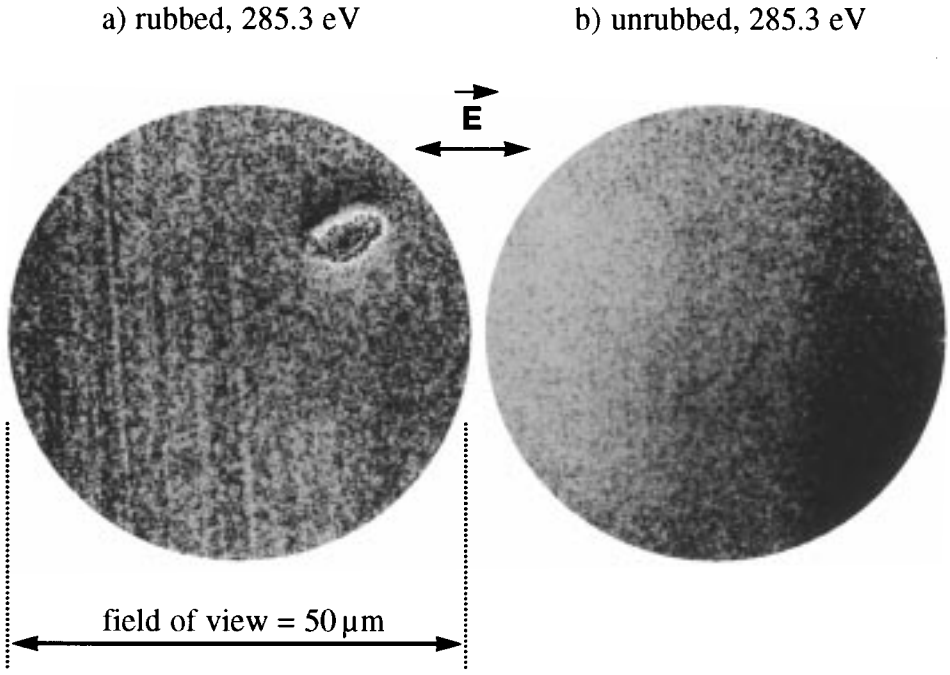

Figure 7. Normalized PEEM images of a rubbed sample in (a) and unrubbed sample in (b) taken at 285.3 eV. The $\vec{E}$ vector was oriented as described by the arrow. The rubbed sample shows the presence of oriented thin lines along the rubbing direction. The rubbing was done vertically.

has been examined by estimating the ratio of the real to apparent contact areas using the contact mechanics theories of roughness described by Johnson[25] and AFM measurements of surface roughness. The surface topography can be approximated either (i) as waves or (ii) as a collection of asperities with Gaussian height distribution as considered by Greenwood and Williamson.[26] Johnson showed that these two approximations give similar results for p^*, the pressure at which the contact is complete. AFM measurements suggest a ratio of amplitude to wavelength of the roughness of about 1500 giving a p^* of about 6 MPa. Therefore, the surface roughness does not influence these results significantly.

Rubbed Samples. X-PEEM imaging was also performed on films rubbed with a velour cloth to examine the spatial homogeneity of the rubbing process. Figure 7 shows two images acquired at the π^* resonance at 285.3 eV. Figure 7a represents the normalized image of a rubbed sample while Figure 7b represents normalized images of a unrubbed sample. Some vertical bright stripes are visible on the rubbed sample indicating the preferential orientation of the phenyl π^* systems perpendicular to the stripes i.e., chain segment orientation parallel to the stripes. The unrubbed sample, Figure 7b, is homogeneous as expected. Neither AFM images nor X-PEEM pictures taken below or far above the C K-absorption edge showed any topological features of similar size, which rules out the possibility that the stripes arise from surface topology. The approximate width of these stripes is several microns which agrees remarkably well with optical measurements of Kikuchi et al.[18] AFM studies showed the presence of much smaller scratches (<0.2 μm width and less than 10 nm in depth) which are due to small hard dust particles. The results shown here clearly show that the rubbing process does not orient the surface of the film homogeneously. However, experiments performed on samples produced under the same conditions showed that liquid crystals are oriented uniformly over the entire sample surface. Thus, the oriented polymer must act as pinning centers to align the liquid crystals. The separation distance between the oriented stripes of polymer is, however, less than the correlation length of the liquid crystal. Consequently, the heteroneneous distribution of the pinning centers is sufficient to fully align the liquid crystals.

Conclusion

X-PEEM is shown to be a versatile tool for examining the orientation of polymer surfaces. It has provided a means of quantitatively assessing the minimal normal stress necessary to provide alignment of the polymer. This is calculated to be 45 MPa, far below the bulk yield stress of 200−300 Mpa of BPDA−PDA. The dichroic ratio $R_{xy} = -0.21$ within the stylized lines is corresponding to the value of -0.2 obtained by Samant et al.[14] from conventional NEXAFS data on sample rubbed with a load of 2 g over a distance of 300 cm. Finally, the X-PEEM results, on rubbed polymers, showed lateral inhomogeneities of the rubbing process which suggests that the oriented regions act as nucleation sites or pinning sites for liquid crystals.

It is, at this point, worthwhile to comment on the implication of the very low value of the normal stress necessary to produce the alignment of the polymer. It may be argued that these data suggest that the glass transition temperatures T_g at the surface is much lower than the bulk value. This would, of course, produce a lower yield stress in keeping with the results found here. However such a dramatic drop in the yield stress would require a substantial drop in the surface T_g and a relaxation of the chain would be expected. This is not observed. These results are also consistents with the arguments of Brown and Russell[11] where a reduction in the entanglement density at the surface of the polymer would be expected due to the conformational restraints placed on the polymer at the surface. Thus, while the polymer chain could be oriented more readily at lower stresses due to the reduced number of entanglements, relaxation would be prohibited since the polymer would still be far below the glass transition temperature.

Acknowledgment. This work was carried out at the SSRL, which is operated by DOE. This work was also supported under the DOE contract DE-AC03-76SF00098 and the NSF Center for Polymer Interfaces and Molecular Assemblies. We also thank the Ministerio de Education y Ciencia of Spain for its financial support.

References and Notes

(1) Depp, S. W.; Howard, W. E. *Sci. Am.* **1993**, *268*, 90.
(2) Geary, J. M.; Goodby, J. W.; Kmetz, A. R.; Patel J. S. *J. Appl. Phys.* **1987**, *62*, 4100.
(3) Van Aerle, N. A. J. M.; Barmentlo, M.; Hollering, R. W. J. *J. Appl. Phys.* **1993**, *74*, 3111.
(4) Berreman, D. W. *Phys. Rev. Lett.* **1972**, *28*, 1683.
(5) Castellano, J. A. *Mol. Cryst. Liq. Cryst.* **1983**, *94*, 33.
(6) Toney, M. F.; Russell, T. P.; Logan, J. A.; Kikuchi, H.; Sands, J. M.; Kumar S. K. *Nature* **1995**, *374*, 709.
(7) Reiter, G. *Europhys. Lett.* **1993**, *23*, 579.
(8) Keddie, J. L.; Jones, R. A. L.; Cory, R. A. *Europhys. Lett.* **1994**, *27*, 59.
(9) Orts, W. J.; van Zanten, J. H.; Wu, W. L.; Satija, S. K. *Phys. Rev. Lett.* **1993**, *71*, 867.
(10) Kajiyama, T.; Tanaka, K.; Takahara, A. *Macromolecules* **1997**, *30*, 280.
(11) Brown, H. R.; Russell, T. P. *Macromolecules* **1996**, *29*, 798.
(12) Meyers, G. F.; DeKoven, B. M.; Seitz, J. T. *Langmuir*, **1992**, *8*, 2330.
(13) Ade, H.; Hsiao, B. *Science* **1993**, *262*, 1427.
(14) Samant, M. G.; Stöhr, J.; Brown, H. R.; Russell, T. P.; Sands, J. M.; Kumar, S. K. *Macromolecules* **1996**, *29*, 8334.
(15) Ade, H.; Zhang, X.; Cameron, S.; Costello, C.; Kirz, J.; Williams, S. *Science* **1992**, *258*, 972.
(16) Cossy-Favre, A.; Diaz, J.; Anders, S.; Padmore, H. A.; Liu, Y.; Samant, M. G., Stöhr, J.; Brown, H. R.; Russell, T. P. *Acta Phys. Polonica A* **1997**, *91*, 923.
(17) Stöhr, J. *NEXAFS Spectroscopy*; Springer Series in Surface Sciences 25; Springer: Berlin, 1992.
(18) Kikuchi, H.; Logan, J. A. Yoon, D. Y. *J. Appl. Phys.* **1996**, *79*, 6811.
(19) Harp, G.; Tonner, B. P. *Proc. Mater. Res. Soc.* **1989**, *143*, 279.
(20) Ree, M.; Yoon, D. Y.; Depero, L. E.; Parish, W. Manuscript in preparation.
(21) Tonner, B. P.; Dunham, D.; Droubay, T.; Pauli, M. *J. Electron Spectrosc. Relat. Phenom.* **1997**, *84*, 211.
(22) Engel, W.; Kordesch, M. E.; Rotermund, H. H.; Kubala, S.; von Oertzen, A. *Ultramicroscopy* **1991**, *36*, 148.
(23) Hertz, H. *Miscellaneous Papers*; Macmillan: London, 1896, p 146.
(24) Johnson, K. L.; Kendall, K.; Roberts, A. D. *Proc. R. Soc. London* **1971**, *A 324*, 301.
(25) Johnson, K. L. *Contact Mechanics*; Cambridge University Press: Cambridge, England, 1985.
(26) Greenwood, J. A.; Williamson, J. B. *Proc. R. Soc. London* **1966**, *A295*, 300.

MA980029B